Statistical mechanics far from equilibrium: prediction and test for a sheared system

R. M. L. Evans,[1] R. A. Simha,[2] A. Baule,[3] and P. D. Olmsted[1]

[1]*School of Physics and Astronomy, University of Leeds, LS2 9JT, U.K.*
[2]*Department of Physics, IIT Madras, Chennai 600 036, India.*
[3]*The Rockefeller University, 1230 York Avenue, New York, NY 10065, U.S.A.*
(Dated: 28 August 2009)

We report the complete statistical treatment of a system of particles interacting via Newtonian forces in continuous boundary-driven flow, far from equilibrium. By numerically time-stepping the force-balance equations of a model fluid we measure occupancies and transition rates in simulation. The high-shear-rate simulation data verify the invariant quantities predicted by our statistical theory, thus demonstrating that a class of non-equilibrium steady states of matter, namely sheared complex fluids, is amenable to statistical treatment from first principles.

Complex fluids relax slowly so their structure is radically re-ordered by flow, as in shear-aligning liquid-crystals [1], jamming suspensions [2], or liposome creation [3]. Sheared fluids consist of particles following the same Newtonian equations of motion as at equilibrium, since no field is applied to drive them; only the boundary conditions differ. Nevertheless, they violate equilibrium statistical mechanics [5], and only the distributions of entropy and work have been rigorously analysed in such cases [6, 7, 8, 11]. In processing and using complex fluids, a state of flux is the rule rather than the exception, e.g. molten plastic flowing into a mould, blood flowing within capillaries, or grease lubricating a rotating axle. Under continuous shear flow, these systems exhibit statistically steady states with intriguing similarities to equilibrium phase behaviour. For example, in "shear-banding" of worm-like micelles [14], the fluid itself partitions the applied shear into a region of low-viscosity *oriented* material at high strain-rate, coexisting with a slower, more viscous region. The parameters controlling this structural phase transition are shear rate and concentration, in addition to temperature. Typically, simplified models with artificial dynamics [16] or near-equilibrium approximations [18] are employed in modelling these types of system, without knowledge of any fundamental principles. Here we validate numerically a complete theory of the detailed statisitics of transition rates and occupancies in a realistic driven system with Newtonian interactions.

We consider a macroscopic region of fluid, our *system*, embedded in a larger volume of the same fluid, which acts as a *heat bath* or *reservoir*, and exerts time-dependent random forces on the system's boundary that are not predictable from a knowledge of the state of the system alone. An instantaneous *microstate* of the system is defined by the exact positions and momenta of all its constituent particles. The laws of motion governing its dynamics can be fully summarized by a set $\{\omega_{ab}\}$ of $\mathcal{N}$ transition rates between every possible pair of microstates a and b that the system can adopt. Here, ω_{ab} is the probability per unit time that the system, currently in microstate a, will be found in microstate b an instant later (so $\omega_{ab} = 0$ for transitions that would violate the laws of motion). In the presence of random impulses from the reservoir, the latter microstate is not uniquely determined. Thus, the set $\{\omega_{ab}\}$ describes *both* the system's dynamics *and* the probability distribution of forces from the reservoir.

Although forces from the reservoir are stochastic, their randomness is nonetheless governed by strict rules. The conditions of thermodynamic *equilibrium* constrain the transition rates to obey the principle of detailed balance (DB), which states that the ratio of forward to reverse transition rates between any pair of microstates must equal the Boltzmann factor of their energy difference, $\omega_{ab}^{\mathrm{eq}}/\omega_{ba}^{\mathrm{eq}} = \exp(E_a - E_b)$ (with microstate energies E_i measured in units of the thermal energy $k_B T$). In other words, the statistical properties of an equilibrium reservoir impose $\mathcal{N}/2$ constraints on the $\mathcal{N}$ rates (one per pair). Equivalently, in a Langevin description of the equilibrium dynamics, the added noise must obey a Fluctuation Dissipation Theorem (FDT) [21] and is Gaussian, with strength determined by the thermodynamic temperature. In a sheared steady state, the system again receives stochastic forces from the reservoir, but with some non-equilibrium distribution; indeed, those forces make the system flow. This generates a different set $\{\omega_{ab}\}$ of transition rates, or equivalently a different noise distribution.

In the absence of a rigorous theory of non-equilibrium statistical mechanics (notwithstanding non-equilibrium generalizations of *thermodynamics* [22]), it has become common practice either to invent the non-equilibrium transition rates, or equivalently to assume that noise obeys the FDT or some other ad hoc criterion (such as colored, *i.e.* time-correlated noise). Although the concept of a non-equilibrium temperature is appealing and has been useful in interpreting non-equilibrium simulations [24], statistical derivations typically make assumptions about microscopic noise or rates [25]. Since arbitrary invention of the rates is forbidden *at equilibrium* by the constraints of DB, one might expect the same degree of constraint to arise also from the statistics of the *sheared* reservoir that influences the *non-equilibrium* rates. Indeed, a non-equilibrium counterpart to DB can be derived from either information-theoretic [26, 27] or Gibbsian [28] arguments, which yield a one-to-one map-

ping between the set of rates $\{\omega_{ab}^{\mathrm{eq}}\}$ in the presence of an equilibrium reservoir, and those $\{\omega_{ab}\}$ for the same system (with the same Hamiltonian) bounded by the sheared steady-state reservoir. The existence of such a mapping means that the driven steady state has the same number of constraints as the equilibrium case, since one may first define an equilibrium system (respecting DB), then apply the mapping to *derive* the driven dynamics.

For completeness, let us briefly discuss the ingredients required to derive the mapping [27, 28]. The transitions are nontrivially correlated via the dynamics so, instead of microstate *transitions*, the basic objects for statistical analysis are *phase-space paths* [29]. Such a path describes a system's entire history of microstates; the position and momentum of every constituent particle at every instant during the very long duration of some steady-state experiment. A phase-space path Γ is therefore a complete description of the real physics exhibited by the system for a particular realisation of the noise, including all existing non-trivial spatial and temporal correlations.

We conceptually construct an *ensemble* of weakly interacting systems that can (i) exchange energy (as in the equilibrium canonical ensemble) and (ii) arbitrarily distribute the total shear strain amongst the member systems (as occurs amongst a set of finite fluid elements within a larger volume of fluid undergoing shearbanding). The crucial property of the phase-space paths of this ensemble is that they are uncorrelated with each other, except via those two quantities (energy and shear strain) that are exchanged over long range due to local conservation laws. Despite this lack of correlation, each path fully describes all the spatial and temporal correlations of its system. We consider all paths consistent with the laws of motion, but differing in their realisations of the noise. For any such set of *uncorrelated* objects, their exact probability distribution p_Γ can be found [31] by maximizing the entropy of that distribution (not to be confused with a thermodynamic entropy) subject to constraints from normalization and conservation laws. The derivation for the sheared case differs from that for equilibrium by only one additional constraint, fixing the ensemble-average of the total shear strain attained by the systems over the duration of the thought-experiment. The result [28] is a relationship between the path distributions in the two ensembles, $p_\Gamma \propto p_\Gamma^{\mathrm{eq}} \exp \nu \gamma_\Gamma$, where ν is a Lagrange multiplier for the extra shear constraint, and γ_Γ is the total strain for path Γ. By summing this relationship over all paths that contain a given transition between a pair of microstates, one obtains the exact mapping, discussed above, between the sets of transition rates $\{\omega_{ab}\}$ and $\{\omega_{ab}^{\mathrm{eq}}\}$. (Supplementary material demonstrates how the same analysis can be used to obtain microstate occupancies, a non-equilibrium analogue of Boltzmann's law.)

We have not stated the one-to-one mapping explicitly here, as it would require further notation to be introduced. However, it was recently noticed [27, 32] that the mapping implies some remarkably simple relationships

that, being exact, apply arbitrarily far from equilibrium. These relationships apply to a state-space with arbitrary connectivity between any set of microstates:

1. The total exit rate from any given microstate differs from its equilibrium value by a shear-rate-dependent constant that is the same for all microstates, i.e. $\sum_b \left(\omega_{ab} - \omega_{ab}^{\mathrm{eq}} \right) = Q(\nu) \; \forall \; a$.

2. The product of forward and reverse transition rates is the same in the equilibrium and sheared ensembles, i.e. $\omega_{ab}\,\omega_{ba} = \omega_{ab}^{\mathrm{eq}}\,\omega_{ba}^{\mathrm{eq}} \; \forall \; a, b$.

We have tested the above theory in a one-dimensional model system, a "fluid" of rotors (see Fig. 1a), each interacting with its neighbours via torsional forces, and respecting Newton's laws of motion. The angular acceleration of each rotor is proportional to its net unbalanced torque, which is the difference between the torques applied by its two neighbours. The torque between neighbours has three contributions: conservative, dissipative and random. The conservative part is the gradient of the four-well potential $U(\Delta\theta)$ shown in Fig. 1b, which is a function of the angular difference between the rotors. Thus, the zero-temperature ground-state has all rotors parallel, but antiparallel and perpendicular configurations are also moderately favourable. The uncorrelated random contribution to the torque (representing any microscopic degrees of freedom that are independent of shear strain, *e.g.* Brownian forces from solvent molecules) has a uniform distribution with width σ and zero mean. The dissipative part is proportional to the difference in angular velocity between neighbours, with a constant of proportionality that can be rescaled to unity without loss of generality, leaving the noise strength σ as the model's only parameter. Neighbours experience equal and opposite torques, so that angular momentum is exactly conserved in the model. The boundary conditions are periodic, and the equations of motion are numerically time-stepped.

As described thus far, this is an equilibrium model. Once initial transients have died away, it exhibits Boltzmann statistics in the occupancies of the potential $U(\Delta\theta)$. At sufficiently low noise strength, the relative angles between neighbours are mostly confined close to the local potential minima, with only occasional transitions between potential wells. The *measured* rates of those transitions respect DB. Note that DB is not imposed *a priori*; it emerges from the dynamics at equilibrium.

We model a fluid under (angular) shear by *twisting* the model (see Fig. 1a). The twist is imposed via the periodic boundary condition, by introducing an offset in the angle measured between rotors either side of the boundary, and increasing that offset linearly in time, at a rate $L\dot\gamma$, so that the twist rate per rotor is $\dot\gamma$. As with ordinary periodic boundary conditions, this angular analogue of Lees-Edwards boundaries [33] avoids edge effects, since it is a non-local condition on the topology of the space; the rotors cannot tell where the boundary is located, as they are only aware of *relative* angles.
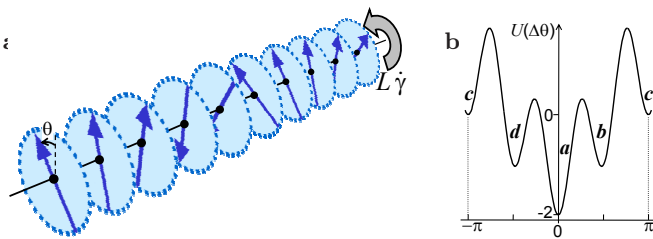
FIG. 1: (a) The one-dimensional rotor model of length L. Each of the L rotors is characterized by its angle θ and angular velocity $\dot{\theta}$. (b) The potential of interaction between neighbours, $U(\Delta\theta) = -\cos\Delta\theta - \cos 4\Delta\theta$, a symmetric periodic function of their angular difference $\Delta\theta$, with four wells, labelled a, b, c, d.

To apply our general theory, some region of the model must be defined as the *system*, while the large remainder is the *reservoir*, supplying unpredictable non-equilibrium forces to it. The system should be much larger than any correlation length, to ensure *weak* coupling to an *uncorrelated* reservoir. Unfortunately, a large system implies a high-dimensional phase space (θ and $\dot{\theta}$ for each rotor), so that acquiring a statistically significant sample of all the transition frequencies becomes prohibitively time-consuming. We take two steps to reduce the phase space. First, we take the limit of small moment of inertia, so that momenta are no longer independent, and the phase space reduces to the set of inter-rotor angles $\Delta\theta$. This has the added advantage, in a one-dimensional force-chain, of reducing the correlation length to zero since, with vanishing rate of change of angular momentum, the forces now balance globally. We are therefore able, secondly, to treat every inter-rotor gap (with its single characteristic variable $\Delta\theta$) as a system, each surrounded by a non-equilibrium reservoir. Note that the general theory applies to systems with non-vanishing correlation lengths, and we are treating a special case only for the sake of expediency. An impediment still exists for analysing this rotor model: the general theory applies to transitions between microstates, whereas the measured transition rates are between potential wells a, b, c and d, that are finite in extent. *If these four continuous sets of microstates are sufficiently analogous to true microstates, then the theory applies in this case.* Subject to that qualification, we can use the model to test the theory's central assumption of *ergodicity*; *i.e.* the available phase-space paths are representatively sampled by the dynamics.

We first test the predicted relationship between exit rates. The required quantity $\sum_a \omega_{ab}^{\rm eq}$ implicitly depends on the unknown temperature of the compared equilibrium system. However, we can eliminate that unknown by appealing to a symmetry of $U(\Delta\theta)$. Since wells b and d are identical *at equilibrium*, they have equal total exit rates, $\omega_{ba}^{\rm eq} + \omega_{bc}^{\rm eq} = \omega_{da}^{\rm eq} + \omega_{dc}^{\rm eq}$. So relationship number 1 predicts them also to have equal total exit rates in the driven case: $\omega_{ba} + \omega_{bc} = \omega_{da} + \omega_{dc}$ *for all* imposed shear rates $\dot{\gamma}$. This equality is not obvious, since the equilib-
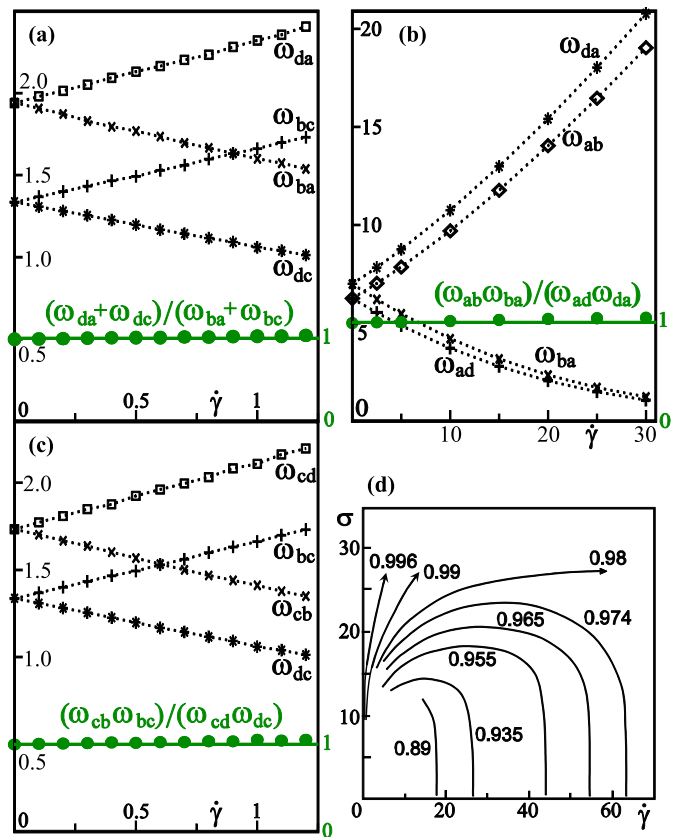

FIG. 2: (a) Test of the prediction $\omega_{da} + \omega_{dc} = \omega_{ba} + \omega_{bc} \ \forall \ \dot{\gamma}$ with noise strength $\sigma = 10$. The left-hand ordinate measures rates, using the same units as the abscissa, while the right-hand ordinate measures the dimensionless ratio. (b) Test of the predicted relationship $\omega_{ab}\,\omega_{ba} = \omega_{ad}\,\omega_{da} \ \forall \ \dot{\gamma}$, with $\sigma = 20$. At this higher noise strength, higher shear rates are numerically accessible because of the greater number of observed backward transitions. (c) Test of the prediction $\omega_{cd}\,\omega_{dc} = \omega_{cb}\,\omega_{bc} \ \forall \ \dot{\gamma}$, for the same parameters as in (a). (d) Contours of the measured ratio $(\omega_{ba} + \omega_{bc})/(\omega_{da} + \omega_{dc})$, predicted to be unity across the whole parameter space of shear rate $\dot{\gamma}$ and noise strength σ. Data acquisition time limited simulations in the bottom left-hand corner. See supplementary material for more data

rium symmetry is broken in the driven case, where one of the potential wells is upstream of the other. Measurements of the four rates in question are plotted against shear rate in Fig. 2a for a particular noise strength. The rates vary considerably with $\dot{\gamma}$ and depart significantly from their equilibrium values. Nevertheless, the ratio of sums, as anticipated, remains very close to unity.

Next we test the second predicted relationship, between products of rates. Again, we exploit the symmetries of the hypothetical equilibrium state to obtain a relationship between the measured rates in the actual driven system only. In *equilibrium*, symmetry of $U(\Delta\theta)$ (together with DB) implies $\omega_{ab}^{\rm eq} = \omega_{ad}^{\rm eq}$ and $\omega_{ba}^{\rm eq} = \omega_{da}^{\rm eq}$. Substitution into proposed relationship 2 implies a constraint on the measured rates in the driven system:

$\omega_{ab}\,\omega_{ba} = \omega_{ad}\,\omega_{da}\ \forall\ \dot{\gamma}$. This prediction is tested in Fig. 2b: as before, while the individual rates vary significantly across the range of driving speeds, the prediction is obeyed to an excellent approximation. Similarly, the equilibrium symmetry about well c gives rise to a third non-equilibrium prediction, $\omega_{cd}\,\omega_{dc} = \omega_{cb}\,\omega_{bc}\ \forall\ \dot{\gamma}$, verified in Fig. 2c.

To quantify the accuracy of the non-equilibrium theory across the model's whole parameter space, contours of the measured ratio $(\omega_{ba} + \omega_{bc})/(\omega_{da} + \omega_{dc})$ are plotted in Fig. 2d. The theory predicts a value of unity everywhere. The small but significant discrepancies between theory and data may be due to the finite extents of the states a, b, c, d, making them not true microstates. Although the non-equilibrium rotor model constitutes an imperfect test of the theory, the theory performs strikingly well here, and exceeds the predictive power of any approximate methods available to non-equilibrium statistical mechanics. Importantly, the discrepancies do not increase with $\dot{\gamma}$, as would be the case for a near-equilibrium theory. The discrepancies at low σ may alternatively be due to failure of the ergodic hypothesis. The theory shares this hypothesis with equilibrium statistical mechanics, which also fails for non-ergodic systems such as glasses, but is successful for a wide range of applications.

While the logistics of data acquisition has restricted our study of the rotor model to the zero-mass, zero-correlation-length limit, the theory should also apply to the more general case with momentum degrees of freedom, thus encompassing phases with non-zero correlation lengths. However, even the testable model studied here exhibits highly non-trivial behaviour, excellently predicted by the non-equilibrium statistical mechanical theory. Of course, no theory can describe *all* non-equilibrium steady states, since such states are much more diverse than the set of all equilibrium problems, for instance encompassing molecular motors, convection cells, granular media and traffic flow. We have nevertheless presented a fundamental theory that governs the steady-state motion of any flowing system on which work is done by a weakly-coupled non-equilibrium reservoir that is ergodic (sufficiently mobile to explore its space of available states thoroughly), and microscopically reversible (containing normal particles with no sense of direction). Such systems include all sheared complex fluids, whose phenomenology is as important to future technologies as it is to our understanding of non-equilibrium physics.

[1] L. A. Archer and R. G. Larson, J. Chem. Phys. **103**, 3108 (1995).

[2] M. D. Haw, Phys. Rev. Lett. **92**, 185506 (2004).

[3] O. Diat and D. Roux, J. Phys. II (France) **3**, 9 (1993).

[4] O. Diat, D. Roux, and F. Nallet, J. Phys. II (France) **3**, 1427 (1993).

[5] L. D. Landau and E. M. Lifshitz, *Statistical Physics* (Butterworth Heinemann, Oxford, 1980).

[6] D. Collin, F. Ritort, C. Jarzynski, S. B. Smith, J. I. Tinoco, and C. Bustamante, Nature **437**, 231 (2005).

[7] J. Liphardt, S. Dumont, S. B. Smith, J. Ignacio Tinoco, and C. Bustamante, Science **296**, 1832 (2002).

[8] C. Jarzynski, Eur. Phys. J. B **64**, 331 (2008).

[9] C. Jarzynski, Phys. Rev. Lett. **78**, 2690 (1997).

[10] G. E. Crooks, Phys. Rev. **E 60**, 2721 (1999).

[11] D. J. Evans, E. G. D. Cohen, and G. P. Morriss, Phys. Rev. Lett. **71**, 3616 (1993).

[12] G. Gallavotti and E. G. D. Cohen, Phys. Rev. Lett. **74**, 2694 (1995).

[13] D. J. Evans and D. J. Searles, Adv. Phys. **51**, 1529 (2002).

[14] S. M. Fielding, Soft Matter **3**, 1262 (2007).

[15] P. D. Olmsted, Rheol. Acta **47**, 283 (2008).

[16] A. Ajdari, Phys. Rev. E **58**, 6294 (1998).

[17] A. Santos, J. J. Brey, and J. W. Dufty, Phys. Rev. Lett. **56**, 1571 (1986).

[18] T. Taniguchi and G. P. Morriss, Phys. Rev. E **70**, 056124 (2004).

[19] J. Casas-Vzquez, M. Criado-Sancho, and D. Jou, Europhys. Lett. **23**, 469 (1993).

[20] K. Kawasaki and J. D. Gunto, Phys. Rev. A **8**, 2048 (1973).

[21] C. W. Gardiner, *Handbook of Stochastic Methods* (Springer, Berlin, 1985).

[22] Y. Oono and M. Paniconi, Prog. Th. Phys. Suppl. **130**, 29 (1998).

[23] S. I. Sasa and H. Tasaki, J. Stat. Phys. **125**, 125 (2006).

[24] T. K. Haxton and A. J. Liu, Phys. Rev. Lett. **99**, 195701 (2007).

[25] L. F. Cugliandolo, J. Kurchan, and L. Peliti, Phys. Rev. E **55**, 3898 (1997).

[26] R. M. L. Evans, Phys. Rev. Lett. **92**, 150601 (2004).

[27] R. M. L. Evans, J. Phys. A **38**, 293 (2005).

[28] A. Simha, R. M. L. Evans, and A. Baule, Phys. Rev. E **77**, 31117 (2008).

[29] G. E. Crooks, Phys. Rev. E **61**, 2361 (2000).

[30] T. S. Komatsu and N. Nakagawa, Phys. Rev. Lett. **100**, 30601 (2008).

[31] F. Mandl, *Statistical Physics* (John Wiley & Sons, Chichester, 1988), 2nd ed.

[32] A. Baule and R. M. L. Evans, Phys. Rev. Lett. **101**, 240601 (2008).

[33] A. W. Lees and S. F. Edwards, J. Phys. C **5**, 1921 (1972).